UCERF3 Appendix E.
Evaluation of Magnitude-Scaling Relationships and Depth of Rupture

Bruce E. Shaw
Lamont Doherty Earth Observatory, Columbia University

Statement of the Problem

In UCERF2 [*WGCEP*, 2008] Magnitude-Area scaling relations contributed one of the main sources of uncertainty in the final hazard estimates. In this task, we seek ways of finding additional constraints or alternative methods of using scaling which will reduce these uncertainties.

Summary of Recommendations

A thorough study was made of the two main uses of magnitude-area relations: one, to figure out the sizes of events, and two, to figure out the rates of events. A previously submitted paper [*Shaw*, 2013] discusses the issues and results more comprehensively. Here, we summarize the preliminary recommendations for UCERF3.

Sizes of Events

Continued use of magnitude-area scaling to estimate sizes of events is recommended. Area based on along-strike length and downdip width remains a good measure. While questions have been raised concerning the depth extent of ruptures during large events, the seismogenic area remains a useful proxy for the purposes of estimating sizes of events.

Regarding which relations to use, four relations are examined here. A fifth relation, the *Somerville* [2006] relation, was rejected based on its dependence on trimmed areas from inverse modeling, which introduces an intermediate step of highly non-unique, model, and smoothing dependent processing of the data.

The four magnitude-area scaling relations examined for estimating sizes of events are as follows. The first is Ellsworth-B:

$$\mathbf{M} = \log A + 4.2 \tag{1}$$

This has the virtue of being extremely simple, being a one parameter fit, and being a good empirical fit to the large earthquake ($\mathbf{M} > \mathbf{6.5}$) data it was developed to fit. The second is *Hanks and Bakun* [2002], a two regime saling:

$$\mathbf{M} = \begin{cases} \log A + 3.98 & A \leq 537\ km^2; \\ \frac{4}{3}\log A + 3.07 & A > 537\ km^2. \end{cases} \tag{2}$$

This has the virtue of doing a better job fitting the data at smaller magnitudes. The third is *Shaw* [2009], which is a generalization of the Hanks and Bakun model; it extends the bilinear Hanks-Bakun two-regime scaling to a three-regime scaling which has a third asymptotic regime valid for very long ruptures $L \gg W$ whereby S approaches W scaling asymptotically. This is done at the price of one additional scaling parameter (the lengthscale at which the transition to the third regime occurs). The *Shaw* [2009] scaling relation is parameterized as follows.

$$\mathbf{M} = log_{10}A + \frac{2}{3}\log_{10}\frac{\max(1, \sqrt{\frac{A}{W^2}})}{(1+\max(1, \frac{A}{W^2\beta}))/2} + const \quad . \tag{3}$$

Here W is the rupture width, and β is a fitting parameter which gives a crossover scale length to the asymptotic W scaling. To match the small events, the constant is set to be the same as in the Hanks-Bakun relation: $const = 3.98$. In the limit of $\beta \to \infty$ the scaling relation reduces to the Hanks-Bakun scaling relation, and in this sense is a one parameter extension of it, if one chooses to treat W as a parameter. Note also that in the limit as $L \to \infty$ it scales asymptotically as $\mathbf{M} \sim \frac{2}{3} log_{10} A$ which gives $S \sim W$, as the *Starr* [1928] and *Knopoff* [1958] solutions suggests. SubAppendix E.2 discusses how the parameters in this scaling relation are determined. For the UCERF3 fault model, $\beta = 7.4$ is a suggested value, with $W = A/L$.

The fourth is a Wells and Coppersmith type linear relations between M and $log_{10} A$

$$\mathbf{M} = C_1 log_{10} A + C_0 \quad . \tag{4}$$

The Ellsworth-B relationship is a special case of these linear relationships, with $C_1 = 1$. Here, the new parameter brings in a new scaling physics. Allowing for a nonspecific parameter on the area term, as the Wells-Coppersmith fitting does, adds substantial complexity to the model, given that it is an exponent on the area. Going from a discrete small set to a continuum is a leap in dimension. It better provide a much better fit to be worth generalizing in such a broad way.

A number of databases were used to compare the scaling laws. Because of concerns about the potential influence of downdip width, the WGCEP03 database containing magnitude, length, and width was used [*WGCEP*, 2003] to calibrate width-sensitive fits, in particular the Shaw09 (S09), Equation (3) relation. The WGCEP03 database is mainly a subset of the *Wells and Coppersmith* [1994] data. The *Hanks and Bakun* [2008] magnitude-area database was used as another target, providing some additional large events and alternative interpretations of areas, particularly at small magnitudes. Finally, supplemental data compiled by *Biasi et al.* [2012] as part of the UCERF3 effort was used as a test of how well the scaling relations fit newer datasets they were not optimized against.

Table 1 shows standard deviations of the fits relative to the data, with the models listed in rank order based on AIC [*Akaike*, 1974]. AIC rewards minimizing errors, while penalizing for extra parameters, and minimum AIC is best. $AIC = -2 \ln \mathcal{L} + 2k$ where $\mathcal{L}$ is the likelihood and k is the number of fitted parameters. Thus differences in AIC correspond to differences in log-likelihood, with relative likelihood of two models being $e^{-\Delta AIC/2}$. This gives a scale of the differences in AIC that matter– at least a few to be significant. AIC is similar to fisher F-Test in that they both examine the importance in the fit relative to the cost of extra parameters. AIC has an advantage in that it doesn't require the lower parameter model to be embedded in the higher parameter one. Used together, standard deviation and AIC provide a helpful view of differences in fits: differences in standard deviation give relative differences in how well the curves are fitting in an absolute sense. Differences in AIC give a sense of how statistically significant, in a log likelihood sense, the differences are.

One issue concerning fits to the data are whether fits across the whole magnitude range or fits just at the large events should be considered, given uncertainties at the small events, but, at the same time, use in hazard calculations of smaller events as well. Both sets of error measures are therefore shown in the table.

Table 1a shows fits to the WGCEP03 data. Table 1b restricts the fits to $\mathbf{M} > 6.5$. Table 1c shows the Hanks-Bakun data, and Table 1d the fits to $\mathbf{M} > 6.5$ for that data. Since only area values are given in the HB database, the Shaw09 relation fixes W as a parameter in fitting that data. Table 1e shows fits to the events added by *Biasi et al.* [2012] as part of the UCERF3 project. This gives a sense of how the models do on events they were not regressed on.

The HB and S09 relations work best across the whole magnitude range, while that EB and S09 work best for just the large events. The original Wells-Coppersmith relation (WC in the table) somewhat underpredicts the Hanks-Bakun dataset at the large events. Refitting the parameters, we find best fitting $C_1 = 1.08$ and $C_0 = 3.86$ ($\text{WC}^\dagger$ in the table). This does a better job. But as we will see

when looking at other types of data, the nonrobustness of the fits (in particular changing C_1 for other different datasets) raises issues for this functional form. When width information is available, the Shaow09 relation using fault based W (denoted S09 in the tables) does better than using fixed values of W (denoted S09′ in the tables), so this is the preferred version of that relation.

Comparing fits of the different scaling laws, in log-log magnitude-log area space, across the whole range of magnitudes ($\mathbf{M} > 5$) the Shaw09 Hanks-Bakun and Modified Wells-Coppersmith type scalings fit better than the Ellsworth-B scaling. For just the large events, ($\mathbf{M} > 6.5$), however, which the EB relation was developed to match, it does quite well. Using as an error metric the difference in magnitude, Fisher F-tests support what we see in AIC: from the lowest magnitudes ($\mathbf{M} > 5$), the S09 relation fits better than the EB relation as does the HB relation relative to the EB relation. But for large magnitudes ($\mathbf{M} > 6.5$), the EB relation begins to do better. At the large magnitudes, the EB, S09, and Modified WC relations are comparable. In contrast, the HB relation begins to do less well. For the whole magnitude range, the S09 relation fits better than the HB relation, significantly in the WGCEP03 data where width information is available, though only just above the level of statistical significance in the Hanks-Bakun data where width data is unavailable and default W values must be used. As the magnitude cutoff increases, the S09 relation does even better against the HB relation. Thus, the extra regime in S09 relative to HB appears justified in terms of a statistically better fit. In fitting the new *Biasi et al.* [2012] data, the EB relation does the best job.

Weighting Recommendation for Sizes of Events

With respect to the weighting, one possibility would be to weight all relations within an acceptable AIC difference equally. Other weightings can also be justified by data uncertainties or theoretical constraints (e.g. a desire for more consistency between scalings used for sizes and rates).

Regarding the Wells-Coppersmith type relations, the original values do not fit well enough at the large magnitudes to justify use. The modified values could be used as a fit to the data. However, non-robustness of parameter fits and difficulty connecting to other data fits, as we will see, are arguments against this branch in a logic tree.

Rates of Events

In UCERF2, rates of events were calculated by moment balancing, with all of the moment from the magnitude-area scaling assumed to occur spread evenly with depth over the seismogenic rupture area. This leads to two major sources of uncertainty. One is the differences in the scaling laws, which have quite different estimated slips for a given area at very large events which dominate the sums in the moment balancing. A second source of uncertainty is the question of whether slip might extend deeper below the seismogenic layer during large events, a question raised by efforts to reproduce scaling laws [*Das*, 1982; *King and Wesnousky*, 2007] by dynamic models [*Shaw and Wesnousky*, 2008] and by kinematic ground motion modeling efforts [*Graves et al.*, 2011]. We propose to address this issue by treating the balancing in terms of slip rate, and expanding the data considered to include geologically observable surface slip data. Slip rate would be targeted to balance at mid-seismogenic depths.

An extensive study of surface slip data and slip-length scaling laws has been carried out and shown to be a viable pathway for inclusion in the slip rate balancing estimates (see preprint submitted in prior report). Qualitative consistency with estimates from magnitude-area scaling was seen, but systematic quantitative differences of order 30% were seen in slip estimated from surface slip measurements, relative to slip estimated from magnitude assuming all the moment occurs over the seismogenic area. Two end member cases are possible. One end member would have the surface slip estimates biased low, with missing slip occurring below measurement detection, perhaps through plastic deformation in unconsolidated sediments. The second end member would have the magnitude-area estimates biased

high, with deeper subseismogenic slip being mapped onto seismogenic depths. Both end members remain possibilities, as does some compromise mixture of a value between the end members involving some amount of both these possible biasing effects. We thus recommend representing both types of estimates in the logic tree.

Implied Slip-Length from Magnitude-Area

Here, we transform magnitude-area scaling into a corresponding implied slip-length scaling. In the moment balancing or slip-rate balancing use of the magnitude-area scaling relations, the slip from each event is summed to get an overall rate of events to match the long-term slip rate on the faults. This slip is summed linearly; as such, it makes sense to see how the scaling laws look not in log-log space, which emphasizes the range of sizes, but in linear-linear space, which emphasizes the largest events which are dominating the sum. To convert the magnitude-area scaling laws to implied slip-length scaling laws, we use the same assumptions involved in doing moment balancing. We convert magnitude $\mathbf{M}$ to moment $\mathcal{M}$ and divide by area A and modulus μ to get slip S: $S = \mathcal{M}/A\mu$. A standard value of the modulus is used ($\mu = 30\ GPa$). Here, we can see the uncertainty in the downdip width playing out: if our area estimates are biased, our slip estimates will be biased. For length and width, we can use the information in databases directly when it is available, as in the WGCEP03 data. Figure 2a shows this transformed data. When it is unavailable, as in the Hanks-Bakun data, we can divide the area by downdip width W to get length L: $L = A/W$. Figure 2b shows this transformation assuming W equals L for small events, but then saturates for large events at the downdip width W. That is, $W = W^*$ where

$$W^* = \min(L, W) = \begin{cases} L & L \leq W; \\ W & L > W \end{cases} \tag{5}$$

with typical values of the seismogenic width $W = 15km$ for vertical strike-slip faults, and downdip widths for dipping faults having correspondingly larger values. Assuming a default downdip width, as in Equation (5), we can infer an L from A. Alternatively, individual values of L from compiled databases (e.g. *Wells and Coppersmith* [1994]) can be used directly with the HB data. We have also checked that when we use individual values of L associated with the events, we get similar results, whether we assume a default value for W and derive an implied L, or we use individual values of L; while individual points do move some, the overall trend is similar. Because of the simplicity and clarity associated with using implied length in conjunction with implied slip, we focus our attention on that approach when using the HB data here.

Again assuming $W = W^*$ the magnitude-area scaling laws transform into slip-length scaling laws as follows. For Ellsworth-B we get

$$S \sim A^{1/2} = C_2(LW^*)^{1/2} = \begin{cases} C_2 L & L \leq W; \\ C_2(LW)^{1/2} & L > W \end{cases} \tag{6}$$

For generalized Wells-Coppersmith type scaling we get

$$S \sim A^{1.5C_1-1} = C_3(LW^*)^{1.5C_1-1} = \begin{cases} C_3 L^{3C_1-2} & L \leq W; \\ C_3(LW)^{1.5C_1-1} & L > W \end{cases} \tag{7}$$

For Hanks-Bakun we get

$$S \sim \begin{cases} (\frac{A}{537})^{1/2} & A \leq 537km^2; \\ \frac{A}{537} & A > 537km^2 \end{cases} = \begin{cases} C_4 L & L \leq W; \\ C_4(LW)^{1/2} & W < L < 537km^2/W; \\ C_4 LW/(537)^{1/2} & 537km^2/W \leq L \end{cases} \tag{8}$$

For Shaw09 we get

$$S \sim \frac{2A/W}{1+\max(1, A/W^2\beta)} = \begin{cases} C_5 L & L \le W\beta; \\ \frac{2C_5}{\frac{1}{L}+\frac{1}{W\beta}} & L > W\beta \end{cases} \tag{9}$$

Taking into account the crossover effects of the finite seismogenic width expressed in Equation (5), we find the magnitude-area scaling laws transformed into slip-length scaling laws are modified to have an additional scaling regime for the Ellsworth-B and Hanks-Bakun scaling, while the Shaw09 scaling ends up actually being reduced by one regime and one parameter, from three to two regimes, and from three to two parameters (C_5 and $W\beta$ in Equation (9)). This reduction for the Shaw09 scaling is not coincidental, since it was developed from a slip-length scaling law.

Comparing the different scalings for large L, we again note very different predicted behaviors. For $L \gg W$ in Hanks-Bakun $S \sim L$, in Ellsworth-B $S \sim L^{1/2}$, and in Shaw09 $S \sim W$. In the generalized WC scaling, $S \sim L^{1.5C_1-1}$, a nonspecific exponent. The scalings also differ in their W dependence at large L, with a linear dependence on W in Hanks-Bakun and Shaw09, and a $W^{1/2}$ dependence in Ellsworth-B. In the generalized WC scaling, $S \sim W^{1.5C_1-1}$, again a nonspecific exponent. Unfortunately, the W values for the data are too uncertain to test the different predicted dependences. Fortunately, the data appear good enough to test some features of the L dependence.

Looking at the fits of the transformed scaling laws to the transformed data in Table 2, the Shaw09 relation is seen to be the best, followed closely by Ellsworth-B, then the Modified WC and then Hanks-Bakun

Surface slip data

Using surface slip data to constrain rates has a number of advantages. First, it manages to avoid some of the uncertainty surrounding the issue of the depth of rupture in large events. Second, it brings into the analysis a new independent geologically observable dataset, thereby bringing in additional testable and collectible information to the estimates. Third, by using slip, which is a linear measure, rather than magnitude, which is a logarithmic measure, as the independent variable, fits to the scaling laws are more naturally mapped onto the linearly summed integral constraints, so errors are better accounted for where they matter most. Finally, it allows for the ability to incorporate pre-instrumental information, opening up the possibility to much extended data sets.

A much more thorough study has been carried out of this approach and has been submitted previously as an accompanying document. Four candidate scalings emerged, The first is a square root $L^{1/2}$ scaling consistent with the implied Ellsworth-B scaling:

$$S \sim A^{1/2} = C_6(LW)^{1/2} \tag{10}$$

This kind of scaling has been proposed by *Leonard* [2010] for large lengths. The second is a linear L scaling consistent with the implied Hanks-Bakun scaling for the largest events:

$$S \sim A = C_7 LW \tag{11}$$

The third is a power law scaling, consistent with the generalized Wells-Coppersmith type scaling. This adds an extra free parameter, a nonspecific exponent η in the scaling, so a much better fit will be needed to make the added model complexity and potential physics worthwhile.

$$S \sim A^{\eta} = C_8(LW)^{\eta} \tag{12}$$

The fourth is a constant stress drop scaling:

$$S = \frac{\Delta\sigma}{\mu}\frac{1}{\frac{7}{3L}+\frac{1}{2W}} \tag{13}$$

with μ the shear modulus and $\Delta\sigma$ the stress drop. This relationship comes from a more careful treatment of how slip would be expected to transition from circular ruptures just beginning to break the surface to long rectangular ruptures. A generalization of the constant stress drop model for dipping faults and oblique slip is added in SubAppendix E.3 [*Shaw*, 2013].

Figure 3 shows the scalings fit to the preliminary UCERF3 Data compiled by *Biasi, Dawson, and Weldon* [2012]. Table 3 shows the fits of the scalings to the data. Table 3a shows the fits to the newer preliminary *Biasi et al.* [2012] data. Table 3b shows the fits to the newer preliminary *Biasi et al.* [2012] California-only data. Table 3c shows the fits to an older data set compiled by *Wesnousky* [2008]. Comparing the fits, the amplitudes found fitting scaling relations to California-only data is around 5-10% smaller than amplitudes found fitting the full new *Biasi et al.* [2012] data. Comparing the old *Wesnousky* [2008] data to the new *Biasi et al.* [2012] data, we see that the amplitudes found from fitting increase around 15%, and the standard deviations increase around 40%, but the overall conclusions remain similar. In both cases the forms trending towards sublinear scaling, where slip which increases less and less as events get longer, substantially outperform the linear scaling model. This is consistent with previous work noting the breakdown in the "L" model scaling for very large aspect ratio events [*Romanowicz*, 1992; *Scholz*, 1994].

Regarding the power law scaling, Equation (12), note in Table 3 that the exponent on the power law scaling isn't very stable with change of dataset, unlike amplitudes of other fits, which covary. The sensitivity of this parameter makes it much less useful as a fitting parameter. This also argues against generalizing to that continuum parameter.

Sublinear Scaling

Both the implied slip versus length and the surface slip versus length curves show sublinear scaling. We find the data very clearly support sublinear scaling, that is increases in slip with length that increase at smaller rates as the lengths get larger. Figure 4 illustrates the sublinear scaling. Figure 4a shows the cumulative slip versus cumulative length, for the data points rank ordered in length. The downward curvature indicates the sublinear scaling. In contrast, linear scaling would imply a constant slope, while upward curvature would imply supralinear scaling. This cumulative curve gives a robust qualitative picture. But the details of the form depend on the density of points along the length axis, so more quantitative measures need a different approach. Figure 4b shows local average slopes in the data. It plots average slope given by average slip divided by average length, versus length. The averages are done over neighboring data points, averaged over $n = 3, 4, 5$ datapoints, represented by different color symbols, in the plot. For the implied slip, in Figure 4b we see, at long lengthscales of $100km$ and more, a systematic decrease in the slope with increasing length. In the plot, we also show with solid lines the implied slopes from magnitude-area curves. We see a good fit for EB and S09, a poor fit functionally for HB, and an underfit for WC to the implied slope from the *Hanks and Bakun* [2008] data.

The sublinear trend is even more evident in the average slope of the surface slip-length data, Figure 4d shows the same type of plot as in Figure 4b, now using surface slip data [*Biasi et al.*, 2012]. The plots also show in solid lines the slopes for the different scaling laws. We see both the $L^{1/2}$ and the constant stress drop models doing well. The constant slope linear fit is again a very poor functional fit. We do not show the power law fit due to sensitivities in the exponents.

Other Scaling Relations

Some other scaling relations have been proposed which we did not explicitly examine here. *Wesnousky* [2008] proposed slip scaling with the log of length. He found the standard deviation for that fit to the data was equivalent to that for an $L^{1/2}$ scaling; given the singularity at 0, the additional

parameter required, and the lack of an extension to a corresponding magnitude-area scaling, we did not consider this to be an additionally worthwhile functional form to pursue. Various authors have proposed generalized Wells-Coppersmith scaling relations (e.g. [*Yen and Ma*, 2011]). *Leonard* [2010] has proposed a set of self-consistent scaling laws based on W scaling with L. In the large L limit it behaves as $L^{1/2}$; at smaller lengths, it has a somewhat different scaling. But given the scatter in the data and the additional parameters associated with changes at smaller scales, the added complexity and added parameters did not appear worth pursuing for the purposes here.

It has long been noted that stable continental regions appear to slip more than plate boundary events– about a factor of 2-3 or so [*Kanamori and Anderson*, 1975; *Scholz*, 1994; *Leonard*, 2010]. Further refinement of catalogues to separate out this effect is one question, and some of the large slip events might be a result of mixing in these type of events. For the surface slip data, the fact that the California-only regressions were only around 5-10% less than the regressions on the global data set suggest this is not a big effect in the catalogues we used. For the implied slip-length data derived from magnitude-area data, this is likely contributing to some of the differences relative to the surface slip data.

Branch recommendations

Four slip-length scaling relations, the two leading implied scalings Equation (1) and Equation (3), and the two leading surface scalings Equations (10) and (13), are shown in Figure 4. The implied slip-length scalings from the magnitude-area scalings are shown with dashed lines, and the slip-length scaling fits to surface slip data are shown in solid lines. We believe that the data do not support the linear scaling of slip with length out to the largest lengths. Moreover, given the sensitivity of the exponents in the power law scaling to the different datasets, and the only marginal improvement in the fitting, we do not believe opening up to nonspecific exponents is justified at this time. We recommend keeping the top two scalings in the two different approaches, which in both the inferred slip-length from magnitude-area and the surface slip-length data show sublinear scaling.

One question regarding the surface slip estiamtes is whether it is better to use a default W, or use fault specific values of W. Because the implied slip estimates from the magnitude-area data already use fault specific values of W, we suggest that a default value of W be used in the surface slip estimates. This approach provides a complementary estimate in the rates which compensates for potential errors in fault specific W estimates. It sacrifices some potential accuracy for instead more robustness and more behavior toward the mean. It gives errors in rates from surface slip with W which are less correlated with errors in the alternative magnitude-area approach. Given uncertainties in W estimates, and the desirability of spanning the range of estimates, using a default W would seem a useful complementary approach on this set of branches. Future study could show sufficient added skill in the W estimates to warrant further use of fault specific W estimates for the rates; but in the absence of sufficiently demonstrated skill, the uncorrelated approach would appear preferable.

Weighting Recommendation for Rates of Events

Sublinear scaling in data disfavors linear $\eta = 1$ scaling. We don't see compelling reason to open up to the continuum, and argue against opening up power law continuum over specific discrete values. There are a number of reasons for this recommendation. We see little if any gain in the arbitrary exponent power law fit over the two discrete exponent fits; and the exponents in the power law change in different data sets. Because exponents are associated with a particular physics, this last feature is especially problematic from a physics-based hazard perspective.

Given the comparability of the fit within the data sets, an equal weighting of the two leading scalings for a given data set is recommended. Given the uncertainty between the branches based on

magnitude-area estimates on the one hand, and the branches based on surface slip-length estimates on the other, an equal weighting between the two different types of estimates would seem a judicious choice. Recommended parameter values would be those in Table 2a and Table 3a. Note that if one wanted to use the California-only rather than the full dataset, Table 3b rather than Table 3a, for consistency some correction for magnitude-area scaling laws should also be made then. Given the small change in best fitting parameter values ($\sim 5-10\%$), we recommend for simplicity using the full dataset, Table 3a.

Weighting Recommendation for Sizes and Rates Combined

Looking for consistency in assumptions underlying the scaling laws used for sizes and the scaling laws used for rates is one way to add additional constraints. This was done implicitly in UCERF2 by using the same scaling laws for the sizes and the events, and not mixing the two laws used. Using this criteria further discourages the use of the continuum power law solutions, since matching power laws on the different data sets would add further nontrivial constraints on physics. It also appears to be sufficiently accounted for in the other sublinear scaling laws. That leaves four clear candidates, if we want compatibility in basic assumptions. One is Equation (1) and Equation (6). A second is Equation (1) and Equation (10). A third is Equation (3) and Equation (9). A fourth is Equation (3) and Equation (13). In the case of the Hanks-Bakun, and associated $\eta = 1$ linear solution, while it is unfavored by the sublinear scaling in the rate estimate fits, and in fits at large events, continuity with its use in previous estimates and its role as an outlier give reasons for including it as a potential branch.

Logic tree recommendation

Table 4 shows the recommended combined branches and parameter values. Table 4a is the full branch sets. A potential trimming of the full branch is shown in Table 4b. An equal weighting of the branches in Table 4a would be one potential recommended approach having the most branches. A trimming based on consistency between functional forms in sizes and rates, as was done in UCERF2, shown in Table 4b, would be an alternative with the fewest branches. Table 4c shows an expansion to include previously used branches.

Hazard Sensitivity Tests to Data Uncertainties

Hazard sensitivities to various model components are of obvious importance to understand. Sensitivity to one data uncertainty could be explored in the following way. A question of whether area estimates of aftershocks may be biased high at the smaller magnitudes [Ellsworth, personal communication, 2009] is something which deserves further observational exploration. While the data side of this is beyond the scope of what can be accomplished in UCERF3, the hazard sensitivity could be tested. Exploration of the hazard significance of deviations in this range could be studied by exploring a range of parameters in the Shaw09 relations, which has the flexibility to change scaling at the small events separately from scaling at the largest events. Thus, for example, comparing the hazard from S09$'$ with ($C_0 = 3.98$, $W = 15km$, $\beta = 7.4$) against S09$'$ with a perturbed set of parameters would be a very good test of hazard sensitivity to the differences in scaling at the small event sizes. Thus, modified parameters ($C_0 + \delta C_0$, $W \cdot 10^{\frac{3}{2}\delta C_0}$, $\beta \cdot 10^{-3\delta C_0}$) with, in particular, $\delta C_0 = .22$ so as to match the scaling of Ellsworth-B at the small events, giving modified parameters ($C_0 = 4.20$, $W = 32.0km$, $\beta = 1.6$) would be an interesting comparison against the unperturbed values. Note that rates will be little impacted by any of this, since slip sums are dominated by the largest events.

Depth Extent of Rupture

Relationship between W and Seismogenic Depth

Past working groups have used the seismogenic depth H as a proxy for downdip width W during large events. However, there is some uncertainty as to what the precise relationship between W and H is. Dynamic ruptures are known to be able to push at least some distance into velocity strengthening layers, so W would be expected to some extent to be at least as large as H. *Rolandone et al.* [2004] found a deepening of seismicity following Landers. We propose to deal with the uncertainty posed by the additional potential deepening with a constant proportionality parameter ξ

$$W = \xi H / \sin\theta \tag{14}$$

In this expression we also have written in explicitly the geometric correction for the fault dip angle θ to transform depth to downdip length. What values are good values to use for ξ needs to be discussed. We can probably put one bound on ξ, since it's unlikely that W would break less deep than H:

$$\xi \geq 1. \tag{15}$$

In principle, ξ need not be a constant, and could be a function of L, implying W being a function of L [*King and Wesnousky*, 2007; *Leonard*, 2010]. This further extension is worthy of additional study. It would, for example, allow the association of the Hanks-Bakun magnitude-area scaling with a sublinear slip-length scaling; one could trade high implied slips instead for high implied downdip widths (though the widths associated with the longest ruptures might be considered problematic). It would, however, lead to additional moment rate estimates for the same slip rates on faults, and since current UCERF3 estimates are already high relative to preferred values, this extension has not yet been examined.

Branch recommendations

In the Tables, we have used W's of $15km$, standard values from aftershock data. A value of $\xi = 1.25$ would be compatable with California observations that $H = 12km$, as well as *Rolandone et al.* [2004]. But weightings in a logic tree to different values of ξ should be discussed, as this parameter has implications for a lot of different things. $\xi = 1$ and 1.5 are two other values to consider.

Coefficients for the regressions to the California-only data, in Table 3b, could also be seen as addressing questions about what W may be relevant. Here, both tectonic differences reflected in stress drops (i.e. intraplate versus interplate) and differences in W might both be expected to tend to increase the global data amplitudes relative to the California-only amplitudes. The fact that there are only 5-10% differences in amplitudes to the the global versus California-only, reflected in the amplitudes in Table 3a compared with Table 3b, suggests that global observations should give a pretty good guide as to what to expect in California.

Faults with substantial surface creep

In locations where surface creep is a substantial fraction of the slip budget, traditional magnitude-area estimates are more appropriate for slip-rate budgeting, and full weighting should be given to those branches of the logic tree. Fortunately, this is a very rare situation for faults. Exceptions in California include the creeping section of the San Andreas Fault, and the Parkfield section and the Hayward Fault, but these exceptions prove the rule, being a very small fraction of the active faults considered in California hazard calculations [*WGCEP*, 2008]. In the case where there is substantial creep, slip estimates that normally would come from surface slip estimates would instead come from magnitude-area estimates. This is because ruptures where lots of surface creep is occurring interseismically are

expected to have altered rupture areas, and potentially different slip from full seismogenic ruptures represented in the surface slip scaling relations. A simple way to do this would be for this to happen when average aseismicity α averaged along a candidate rupture is above a critical threshold:

$$< \alpha >= \frac{1}{L} \int_0^L \alpha(x) dx \geq \alpha_c \tag{16}$$

with $\alpha_c = .2$ being a recommended value. Other values of α_c which could be tried include .15 and .3. We do not expect more than small impacts on hazard estimates from this choice.

Other Issues Regarding the Depth Extent of Rupture

Variable Width Dip-Slip Faults

Our scaling relations were formulated in terms of a downdip seismogenic width W. When this width varies along-strike, the relevant quantity is the average width (to leading order is the arithmetic average W which matters in constant stress drop scalings [*Shaw*, 2009]). With respect to UCERF, which has variable $W's$ in its database, there are two ways to deal with varying W. One way is to take the seismogenic widths as given in the fault database, and calculate an arithmetic average over candidate length L ruptures. This assumes that the variation in the widths in the database are relatively well known beyond just dip information, and that varying seismogenic depth on dipping faults is sufficiently constrained to make the added information useful to incorporate. The second way is to presume the most homogeneous case and make minimal demands on observations, by assuming a constant seismogenic depth, and assume all width variations come from dip variations. Both these two ways of doing things are straightforward to implement. It would be useful to do them both, and compare the results. Which one would be favored from a branch weight point of view depends on how much confidence there is in deviations of seismogenic depths on dip slip faults relative to default values, and the relationships to downdip rupture.

Physics based ground motion simulators

The depth extent of rupture is relevant not only to helping constrain slips and rates in events, but also as input constraints for statistically based kinematic models of ruptures. A variety of such models have been developed (e.g. [*Herrero and Bernard*, 1994; *Mai and Beroza*, 2000]). These kinds of models have been used recently in an effort to use statistically based kinematic models to forward model ground motions. In the Cybershake case [*Graves et al.*, 2011], the goal is to get a better estimate of ground motions and hazard in geographically specific settings, replacing ground motion prediction equations, which relate shaking levels to various rupture parameters such as magnitude and closeness of rupture in generic settings, with geographically specific basin and directivity effects from ensembles of ruptures for particular velocity models and rupture distributions.

Cybershake [*Graves et al.*, 2011] is somewhat outside the scope of UCERF3, but it is, nevertheless an interested user, and potentially could develop into a useful constraint, feeding back on the scaling laws as a consistency check. We thus focus our attention on it here in this discussion.

Initial efforts in Cybershake have run into difficulties combining magnitude-area scaling laws used in UCERF2 with particular kinematic models to match some features of GMPE's. Whether the issues are associated with the scaling laws, the particular kinematic models, the GMPE's, or some combination of these effects is still an open question and area of active research. Here, we offer a few remarks from the scaling side of things hopefully of relevance to Cybershake and other kinematic modeling efforts.

Since Cybershake itself has many underlying assumptions (such as the degree of coherence in the ruptures), sensitivities in Cybershake need to be explored further before it is used as a constraint on UCERF relations. Nevertheless, it is a goal to have compatibility developed, and thus exploring the implications of the various relations in this context is an important task.

An unresolved epistemic uncertainty in the depth dependence of slip concerns how much coseismic slip may be occurring below the seismogenic layer. Dynamic models suggest a significant fraction of slip may be occurring below the seismogenic layer– up to of order 1/3 the total moment [*Shaw and Wesnousky*, 2008]. This slip would be occurring mainly as long period motion, with a dearth of high frequencies [*Shaw and Wesnousky*, 2008].

An exponential decay or a linear decay with depth below the seismogenic layer are both reasonable parameterizations of what is seen in the dynamic models [*Shaw and Wesnousky*, 2008]. The scale length of the decay depends on the degree of velocity strengthening; the degree of strengthening is not well constrained, and thus the scale length remains an epistemic uncertainty.

The distributions of slip, and rupture velocities, are important factors which warrant further study in Cybershake. Correlations of slip at the surface have gaussian, or even faster than gaussian falloff in the tails [*Shaw*, 2011], so Cybershake simulations positing extreme slip values in the distributions (e.g. $50m$ slip in great strike-slip earthquake patches) should be reexamined. Recent LIDAR measurements of surface offsets in California confirm this dearth of very high slip values.

Given the implied high stress drops at moderate magnitudes in the Ellsworth-B relations, and the implied high stress drops at large magnitudes in the Hanks-Bakun relations, it would be interesting to see if constant stress drop models can be seen to be compatible with Cybershake. Is, for example, the Shaw09 magnitude-area scaling relation, combined with a 30% subseismogenic high-frequency deficient moment, compatible with more high variance rupture velocity low variance slip patch versions of Cybershake?

References

Akaike, H., A new look at the statistical model identification, *IEEE Transactions on Automatic Control*, *AC19*, 716, 1974.

Biasi, G., T. Dawson, and R. Weldon, Preliminary event data for ucerf3, *private communication*, 2012.

Das, S., Appropriate boundary-conditions for modeling very long earthquakes and physical consequences, *Bull. Seismol. Soc. Am.*, *72*, 1911, 1982.

Graves, R., et al., Cybershake: A physics-based seismic hazard model for Southern California, *Pageoph*, *168*, 367, 2011.

Hanks, T. C., and W. H. Bakun, A blinear source-scaling model for M-log A observations of continental earthquakes, *Bull. Seismol. Soc. Am.*, *92*, 1841, 2002.

Hanks, T. C., and W. H. Bakun, M-log A observations of recent large earthquakes, *Bull. Seismol. Soc. Am.*, *98*, 490, 2008.

Herrero, A., and P. Bernard, A kinematic self-similar rupture process for earthquakes, *Bull. Seismol. Soc. Am.*, *84*, 1216, 1994.

Kanamori, H., and D. L. Anderson, Theoretical basis for some empirical relations in seismology, *Bull. Seismol. Soc. Am.*, *65*, 1073–1095, 1975.

King, G. L., and S. Wesnousky, Scaling of fault parameters for continental strike-slip earthquakes, *Bull. Seismol. Soc. Am.*, *97*, 1833, 2007.

Knopoff, L., Energy release in earthquakes, *Geophys. J. R. A. S.*, *1*, 44, 1958.

Leonard, M., Earthquake fault scaling: Self-consistent relating of rupture length, width, average displacement, and moment release, *Bull. Seismol. Soc. Am.*, *100*, 1971, 2010.

Mai, P. M., and G. C. Beroza, Source scaling properties from finite rupture models, *Bull. Seismol. Soc. Am.*, *90*, 604–615, 2000.

Rolandone, F., R. Bürgmann, and R. M. Nadeau, The evolution of the seismic-aseismic transition during the earthquake cycle: Constraints from the time-dependent depth distribution of aftershocks, *Geophys. Res. Lett.*, *31*, L23,610, 2004.

Romanowicz, B., Strike-slip earthquakes on quasi-vertical transcurrent fault: inferences for general scaling relations., *Geophys. Res. Lett.*, *19*, 481, 1992.

Scholz, C. H., Reply to comments on 'A reappraisal of large earthquake scaling, *Bull. Seismol. Soc. Am.*, *84*, 1677–1678, 1994.

Shaw, B. E., Constant stress drop from small to great earthquakes in magnitude-area scaling, *Bull. Seismol. Soc. Am.*, *99*, 871, 2009.

Shaw, B. E., Surface slip gradients of large earthquakes, *Bull. Seismol. Soc. Am.*, *101*, 792, 2011.

Shaw, B. E., Earthquake surface slip length data is fit by constant stress drop and is useful for seismic hazard analysis, *Bull. Seismol. Soc. Am.*, 2013.

Shaw, B. E., and S. G. Wesnousky, Slip-length scaling in large earthquakes: The role of deep penetrating slip below the seismogenic layer, *Bull. Seismol. Soc. Am.*, *98*, 1633, 2008.

Somerville, P. G., Review of magnitude-area scaling of crustal earthquakes, *Rep. to WGCEP*, 2006.

Starr, A. T., Slip in a crystal and rupture in a solid due to shear, *Proc. Camb. Phil. Soc.*, *24*, 489, 1928.

Wells, D. L., and K. J. Coppersmith, New empirical relationships among magnitude, rupture length, rupture width, rupture area, and surface displacement, *Bull. Seismol. Soc. Am.*, *84*, 974, 1994.

Wesnousky, S. G., Displacement and geometrical characteristics of earthquake surface ruptures: Issues and implications for seismic-hazard analysis and the process of earthquake rupture, *Bull. Seismol. Soc. Am.*, *98*, 1609, 2008.

WGCEP, Earthquake probabilities in the San Francisco Bay Region: 2002 to 2031, *U.S. Geol. Surv. Open File Rep., 03-214*, 2003.

WGCEP, The Uniform California Earthquake Rupture Forecast, version 2 (UCERF2), *U.S. Geol. Surv. Open File Rep., 2007-1437*, 2008.

Yen, Y. T., and K. F. Ma, Source-scaling relationship for M 4.6-8.9 earthquakes, specifically for earthquakes in the collision zone of Taiwan, *Bull. Seismol. Soc. Am.*, *101*, 468, 2011.

SubAppendix E.1: Fits of Scalings to Data

Magnitude-Area Scaling

The standard deviation in the above table measures the difference in magnitudes of the data from the predicted curve. A least squares fit is done, which neglects errors in area relative to errors in magnitude. The number of free parameters is given by No., with the best fitted parameter values following that. The parameter C_0 is the constant in the magnitude-area scaling relations. Ranking in this table, and those that follow, is by minimum AIC [*Akaike*, 1974], which rewards reduced standard deviation but penalizes additional parameters. $AIC = -2\ln\mathcal{L} + 2k$ where $\mathcal{L}$ is the likelihood and k is the number of fitted parameters. Thus differences in AIC correspond to differences in log-likelihood, with relative likelihood of two models being $e^{-\Delta AIC/2}$. This gives a scale of the differences in AIC that matter– at least a few to be significant. In the table we use $AIC = n(\ln(2\pi\sigma^2) + 1) + 2k$ where σ is the std dev and n the number of data points and again k the number of parameters. (a) Data from WGCEP03 database [*WGCEP*, 2003]. The modified WC scaling is denoted with a dagger symbol: WC†. The S09 scaling with fixed values of W is denoted with a prime symbol: S09$'$. (b) Only large magnitudes $M > 6.5$ are considered, reducing the number of data points from 77 to 49. Because the parameters are not refit to the reduced data set, we mark the AIC with a star, AIC*, to indicate the parameter penalties are perhaps overly harsh, since the parameters are not refit. But the AIC values do give some help as to the statistical significance of the differences in the standard deviations, so they are presented nevertheless. This way of doing things favors to some degree the EB scaling, since it was designed to fit over this range, while the other scalings were fit over the whole range. (c) Data from the Hanks-Bakun database [*Hanks and Bakun*, 2008]. Because width information is unavailable, only S09$'$ fixed W solutions are shown. Two of those are shown; one optimized for the Hanks-Bakun data, and the other a default version based on the WGCEP03 data. (d) Only large magnitudes $M > 6.5$ are considered, reducing the number of data points from 87 to 36. Again, this favors the EB scaling. (e) Misfits to new events in the *Biasi et al.* [2012] database. Formal uncertainties in the parameter fits are at the 10% level in the different tables.

Table 1: Magnitude-Area Scaling Fits

(a) Fits to complete WGCEP03 magnitude-area-width dataset

Scaling		Best fits		Parameters			
Name	Eqn	Std. dev.	AIC	No.	Best fit values		
S09	(3)	.202	-23.62	2	$C_0 = 3.98$	$\beta = 7.4$	
WC†	(4)	.203	-22.87	2	$C_0 = 3.89$	$C_1 = 1.08$	
S09′	(3)	.204	-20.65	3	$C_0 = 3.98$	$\beta = 7.4$	$W = 15\ km$
HB	(2)	.212	-16.13	2	$C_0 = 3.98$	$A_c = 537\ km^2$	
WC	(4)	.217	-12.50	2	$C_0 = 3.98$	$C_1 = 1.02$	
EB	(1)	.229	-6.15	1	$C_0 = 4.20$		

(b) Misits to $M > 6.5$ subset of WGCEP03 data without refitting parameters

Scaling		Misfits $M > 6.5$		Parameters			
Name	Eqn	Std. dev.	AIC*	No.	Values		
EB	(1)	.173	-31.09	1	$C_0 = 4.20$		
S09	(3)	.177	-26.23	2	$C_0 = 3.98$	$\beta = 7.4$	
WC†	(4)	.178	-26.32	2	$C_0 = 3.89$	$C_1 = 1.08$	
S09′	(3)	.190	-17.60	3	$C_0 = 3.98$	$\beta = 7.4$	$W = 15\ km$
HB	(2)	.213	-8.72	2	$C_0 = 3.98$	$A_c = 537\ km^2$	
WC	(4)	.216	-7.17	2	$C_0 = 3.98$	$C_1 = 1.02$	

(c) Fits to complete Hanks-Bakun magnitude-area dataset

Scaling		Best fits		Parameters			
Name	Eqn	Std. dev.	AIC	No.	Best fit values		
S09′	(3)	.208	-20.54	3	$C_0 = 3.98$	$\beta = 5.0$	$W = 19\ km$
HB	(2)	.213	-18.46	2	$C_0 = 3.98$	$A_c = 537\ km^2$	
WC†	(4)	.215	-16.43	2	$C_0 = 3.86$	$C_1 = 1.08$	
S09′	(3)	.213	-15.78	3	$C_0 = 3.98$	$\beta = 7.4$	$W = 15\ km$
WC	(4)	.220	-12.32	2	$C_0 = 3.98$	$C_1 = 1.02$	
EB	(1)	.275	24.23	1	$C_0 = 4.20$		

(d) Misfits to $M > 6.5$ subset of Hanks-Bakun data without refitting parameters

Scaling		Misfits $M > 6.5$		Parameters			
Name	Eqn	Std. dev.	AIC*	No.	Values		
EB	(1)	.185	-17.26	1	$C_0 = 4.20$		
WC†	(4)	.193	-12.21	2	$C_0 = 3.86$	$C_1 = 1.08$	
S09′	(3)	.200	-7.58	3	$C_0 = 3.98$	$\beta = 5.0$	$W = 19\ km$
S09′	(3)	.204	-6.32	3	$C_0 = 3.98$	$\beta = 7.4$	$W = 15\ km$
HB	(2)	.213	-5.27	2	$C_0 = 3.98$	$A_c = 537\ km^2$	
WC	(4)	.216	-4.05	2	$C_0 = 3.98$	$C_1 = 1.02$	

(e) Misfits to new *Biasi et al.* [2012] magnitude-area-width data without refitting parameters

Scaling		Best fits		Parameters			
Name	Eqn	Std. dev.	AIC*	No.	Best fit values		
EB	(1)	.145	-17.34	1	$C_0 = 4.20$		
S09	(3)	.165	-10.65	2	$C_0 = 3.98$	$\beta = 7.4$	
WC†	(4)	.175	-8.24	2	$C_0 = 3.86$	$C_1 = 1.08$	
WC	(4)	.210	-1.27	2	$C_0 = 3.98$	$C_1 = 1.02$	
HB	(2)	.234	2.69	2	$C_0 = 3.98$	$A_c = 537\ km^2$	

Slip-Length Scaling from Implied Magnitude Area Data

Table 2: Implied Slip-Length from Magnitude-Area

(a) Misfits without rescaling for new metric; from WGCEP03 data

Scaling		Unrescaled Misfit		Parameters		
Name	Eqn	Std. dev.	AIC*	No.	Values	
S09	(3)	1.212	252.1	2	$C_0 = 3.98$	$\beta = 7.4$
S09′	(3)	1.245	256.3	2	$C_0 = 3.98$	$W\beta = 15 * 7.4 = 111\ km$
EB	(1)	1.275	258.0	1	$C_0 = 4.20$	
WC†	(4)	1.415	276.0	2	$C_0 = 3.86$	$C_1 = 1.08$
HB	(2)	1.687	303.0	2	$C_0 = 3.98$	$A_c = 537\ km^2$
WC	(4)	1.699	304.1	2	$C_0 = 3.98$	$C_1 = 1.02$

(b) Misfits without rescaling for new metric; from *Hanks and Bakun* [2008] data

Scaling		Unrescaled Misfit		Parameters		
Name	Eqn	Std. dev.	AIC*	No.	Values	
S09′	(3)	1.180	279.6	2	$C_0 = 3.98$	$W\beta = 15 * 7.4 = 111\ km$
EB	(1)	1.211	282.2	1	$C_0 = 4.20$	
WC†	(4)	1.282	294.1	2	$C_0 = 3.86$	$C_1 = 1.08$
HB	(2)	1.459	316.6	2	$C_0 = 3.98$	$A_c = 537\ km^2$
WC	(4)	1.549	327.0	2	$C_0 = 3.98$	$C_1 = 1.02$

(c) Surface Slip scaling relations fit to Hanks-Bakun implied slip-length data

Scaling		Best fits		Parameters		
Name	Eqn	Std. dev.	AIC	No.	Best fit values	
L^η	(12)	1.190	281.1	2	$C_8 = 0.026$	$\eta = .632$
$L^{1/2}$	(10)	1.236	285.8	1	$C_6 = 7.46 \cdot 10^{-5}$	
S12	(13)	1.249	287.6	1	$\Delta\sigma = 5.95\ MPa$	
L	(11)	1.339	299.7	1	$C_7 = 1.19 \cdot 10^{-6}\ km^{-1}$	

The standard deviation in the above table measures the difference in slip of the data from the predicted curve. The data are transformed from magnitude-area to slip-length as follows. To get slip we convert magnitude to moment and divide by area and modulus to get slip. When length is available we use it. When it is not, we divide area by a default width, with width being the lesser of the length compared with with downdip seismogenic width. To get length we divide area by width, assuming width is the lesser of the length compared with the downdip seismogenic width. Note that we do not refit the parameters, which were set based on fits in log space magnitude-log area, to the new linear space slip-length metric. As previously, when we do not refit the parameters, with denote this with AIC*. (a) Transformed data from WGCEP03 data [*WGCEP*, 2003]. Lengths from database. (b) Transformed data from Hanks-Bakun database [*Hanks and Bakun*, 2008]. Lengths from dividing area by default width, with seismogenic width of $15km$. (c) Surface slip-length scaling relations are fit to the implied slip-length Hanks-Bakun data. This is done for completeness, and comparison with the surface slip-length data. Formal uncertainties in parameter fits are at the 10% level in the different tables.

Slip-Length Scaling from Surface Slip Data

Table 3: Slip-Length from Surface Slip Data

(a) Fits to new [*Biasi et al.*, 2012] data

Scaling		Best fits		Parameters		
Name	Eqn	Std. dev.	AIC	No.	Best fit values	
S12	(13)	1.12	139.6	1	$\Delta\sigma = 4.54\ MPa$	
L^η	(12)	1.11	141.4	2	$C_8 = 0.142$	$\eta = .387$
$L^{1/2}$	(10)	1.14	141.5	1	$C_6 = 5.69 \cdot 10^{-5}$	
L	(11)	1.52	167.1	1	$C_7 = 8.10 \cdot 10^{-7}\ km^{-1}$	

(b) Fits to new [*Biasi et al.*, 2012] California-only data

Scaling		Best fits		Parameters		
Name	Eqn	Std. dev.	AIC	No.	Best fit values	
S12	(13)	.659	34.0	1	$\Delta\sigma = 4.14\ MPa$	
$L^{1/2}$	(10)	.666	34.4	1	$C_6 = 5.33 \cdot 10^{-5}$	
L^η	(12)	.664	36.3	2	$C_8 = 0.066$	$\eta = .474$
L	(11)	1.08	49.8	1	$C_7 = 8.02 \cdot 10^{-7}\ km^{-1}$	

(c) Surface Slip scaling relations using adapted older [*Wesnousky*, 2008] data.

Scaling		Best fits		Parameters		
Name	Eqn	Std. dev.	AIC	No.	Best fit values	
S12	(13)	.760	50.05	1	$\Delta\sigma = 3.91\ MPa$	
$L^{1/2}$	(10)	.804	52.43	1	$C_6 = 4.91 \cdot 10^{-5}$	
L^η	(12)	.788	53.60	2	$C_8 = 0.093$	$\eta = .421$
L	(11)	1.174	68.34	1	$C_7 = 7.10 \cdot 10^{-7}\ km^{-1}$	

The standard deviation in the above table measures the difference in slip of the data from the predicted curve. The table shows a comparison of the surface slip data with scaling relations proposed for surface slip-length scaling. (a) Fits to new *Biasi et al.* [2012] preliminary data. There are 45 data points in the fit to the strike-slip data. The best overall fit to the data, in terms of AIC, is S11, the constant stress drop model, Equation (13), followed closely by the $L^{1/2}$ model, Equation (10). (b) Fits to new *Biasi et al.* [2012] preliminary California-only data. In this case, there are only 16 data points. Leaving aside the power law fit, the best fitting parameters change only slightly, being about 5-10% lower in amplitude than the full dataset. The top models remain close, but swap places a little. The scatter is also reduced in this restricted dataset. (c) Fits to the older [*Wesnousky*, 2008] data. Again leaving aside the power law fit, the main change for the new fits relative to the old fits are that the amplitude of the fits increase around 15% with the new data, and the scatter, reflected in the standard deviation, increases around 40%. With respect to the power law fits across the different data sets, note the parameter sensitivity of η to the datasets. This is an undesirable quality of a measure, and this argues against the extension of dimension in this direction. In contrast, the covariance of the fits $L^{1/2}$, S12, and L to the different datasets is substantial; they are stably varying together.

Branches in Logic Tree

Table 4: Logic Tree Branches

(a) Full branches

Sizes			Rates		
Name	Eqn	Table	Name	Eqn	Table
S09	(3)	1a	S09	(9)	2a
			EB	(6)	2a
			S12	(13)	3a
			$L^{1/2}$	(10)	3a
EB	(1)	1a	S09	(9)	2a
			EB	(6)	2a
			S12	(13)	3a
			$L^{1/2}$	(10)	3a
HB	(2)	1a	S09	(9)	2a
			EB	(6)	2a
			S12	(13)	3a
			$L^{1/2}$	(10)	3a
WC†	(4)	1c	S09	(9)	2a
			EB	(6)	2a
			S12	(13)	3a
			$L^{1/2}$	(10)	3a

(b) Trimmed by consistency of scaling assumption

Sizes		Rates	
Name	Eqn	Name	Eqn
S09	(3)	S09	(3)
		S12	(13)
EB	(1)	EB	(1)
		$L^{1/2}$	(10)

(c) Extension of consistency set to previously used branch

Sizes			Rates		
Name	Eqn	Table	Name	Eqn	Table
S09	(3)	1a	S09	(3)	1a
			S12	(13)	3a
EB	(1)	1a	EB	(1)	1a
			$L^{1/2}$	(10)	3a
HB	(2)	1a	HB	(2)	1a

Tables showing branches in logic tree. (a) Maximal branches showing four viable magnitude-area scaling laws combined with four viable slip-length scaling laws, for a total of 16 branches. (b) Trimmed set of branches using consistency in scaling assumptions, having basis of scaling in sizes be consistent with same assumptions underlying scaling in rates. This type of consistency was used in UCERF2. (c) Extension of trimmed consistency set to include previously used branch which also provides role as outlier. Note: default values unless otherwise specified are $W = 15km$. Also $\mu = 30\ GPa$.

SubAppendix E.2: Parameters for Shaw09 Scaling Relation

The Shaw09 (S09) parameters in Equation (3) are set as follows. Because the S09 relation is meant to generalize the Hanks-Bakun relation, we fix the constant parameter to equal the constant in the Hanks-Bakun relation. This is not necessary, but uncertainties in the constant parameter are dominated by uncertainties in area estimates at small magnitudes, and no additional progress on this issue has been made on this issue since the last UCERF report, so we stick with continuity.

As we discuss further elsewhere in the report, substantial uncertainty exists concerning the relationship of seismogenic depth and rupture width. Because of these uncertainties, and because the S09 parameters use width information, we calibrate the parameters in a way which aims to best reproduce similar treatments of the inputs. The WGCEP03 database contains width information, so we use that to calibrate the S09 β parameter.

The width W can be treated either as a fixed value and thus as a parameter in the S09 relation, or as input from a given rupture. The advantage of using it as input is that it allows for a broader range of applicability beyond the fixed value. It is also found to do a better job fitting the data. Nevertheless there are instances where one may want it to have a default value, such as when one wants to examine sensitivities and uncertainties in W estimates, or when width information is unavailable, as it is in the Hanks-Bakun database which just has magnitude and area.

To find a default β value, we fix W, since pre-event area based on seismogenic depth is more akin to a default W value. The UCERF3 fault database has an average W around $11km$, so we take that as the fixed value. To avoid mixing in substantially bigger W's, we restrict the WGCEP03 dataset on which we fit β to $W < 15km$. For these events with widths comparable to California events we obtain for $W = 11km$ a best fit $\beta = 7.4$ using least squares magnitude misfits. There is quite a broad minimum, and other values could also be used with little degradation in misfit. This does, however, give a means of fixing a value for β, and if it does a good job on other datasets, it will be a satisfactory parameter choice.

For the Hanks-Bakun dataset, since only area is provided, a fixed value of W is used. We use a default value of $W = 15km$ for this global dataset, which includes some ruptures believed to be much wider than typical values for California faults. A good job fitting the data would indicate this is a reasonable choice.

SubAppendix E.3: Dipping faults

The constant stress drop model has been generalized for dipping faults and oblique slip.

For dip-slip faults, two effects impact the scaling. One effect is that the downdip width W is generally larger for dipping faults, as Equation (14) shows. For dips of 90° (strike-slip), 60° (normal), and 30° (thrust), the factor $1/\sin\theta$ is, respectively, 1, 1.15, and 2. Thus only for quite shallow dips is this a significant factor. A second factor is a change in the coefficient on W for the infinite rupture, with the factor of 2 replaced by $(\lambda + 2\mu)/(\lambda + \mu) = 1/(1 - (v_s/v_p)^2)$ where v_s/v_p is the ratio of the shear wave speed to the compressional wave speed. Using typical values of v_p/v_s of 1.75 gives typical values around 1.5 for this factor or about 3/4 of the value for dip-slip relative to strike-slip. Thus, for dip-slip cases, we have

$$S = \frac{\Delta\sigma}{\mu} \frac{1}{\frac{7}{3L} + \frac{1}{\left(\frac{\lambda+2\mu}{\lambda+\mu}\right)W}} \tag{17}$$

We can further generalize this to the oblique slip case for slip in the arbitrary direction $\hat{s}$ consisting of along-strike and dip-slip components:

$$S = \frac{\Delta\sigma}{\mu} \frac{1}{\frac{7}{3L} + \frac{1}{W\hat{s}\cdot\left(2, \frac{\lambda+2\mu}{\lambda+\mu}\right)}} \tag{18}$$

Figure 6 shows these combined effects for the three dip cases, of $\theta = 90°$ using Equation (13), and $\theta = 60°$ and 30° using Equation (17), assuming constant seismogenic depth and correspondingly varying downdip W, and with the later two dip-slip cases including the modulus effect in Equation (17).

We see the modulus effect beating the increased W effect at 60°, so the expected slip is slightly lower for the 60° dip case. The crossover where the two effects are comparable occurs around 45°. By 30° the increased W effect dominates and slip is indeed increased, but not by a huge amount. It is really not until we get to very shallowly dipping faults that a whole new scale of slip enters in, at dips and W's relevant to subduction zones. Thus, for subareal surface rupturing events, under constant stress drop scaling we expect not very different slips for dip-slip versus strike-slip events. And the data, sparse as it is, appears to support this. The conclusion that dip-slip events have similar stress drops as strike-slip events has also been found in regressions using other types of scaling assumptions [*Leonard*, 2010]. This lends additional support to the approach of treating dip-slip and strike-slip events similarly.

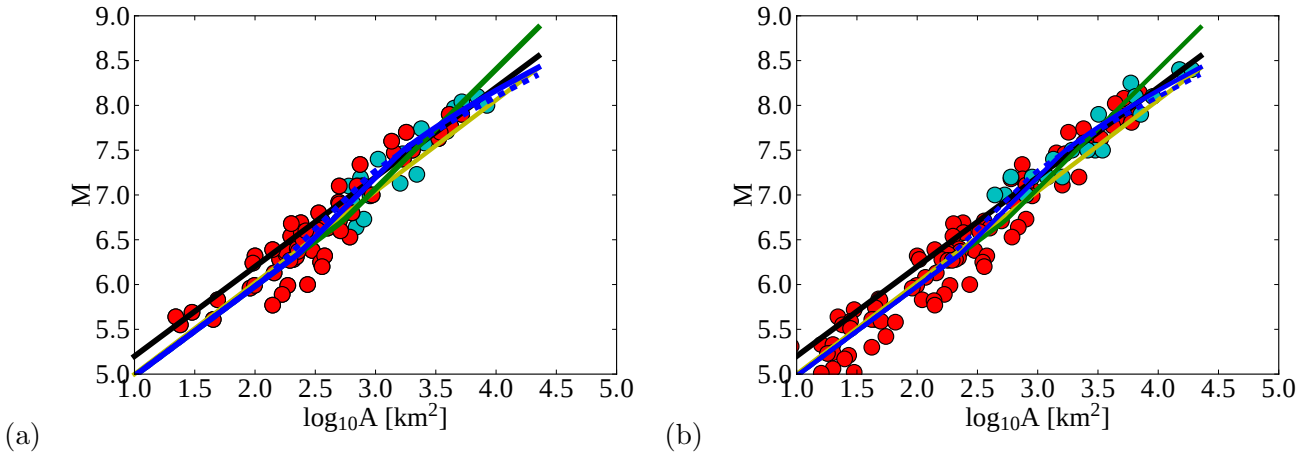

Figure 1: Magnitude area relations for large strike-slip events. (a) WGCEP03 data. Red circles denote $W < 15km$ events, cyan circle denote $W > 15km$ events. (b) Red circles denote magnitude and area of events from *Hanks and Bakun* [2008] database. Cyan circles from *Biasi et al.* [2012] database. Curves are fit to *Hanks and Bakun* [2008] database, with *Biasi et al.* [2012] data shown for comparison. Black line is linear Ellsworth-B [*WGCEP*, 2003] magnitude-area relation, Equation (1). Green line is *Hanks and Bakun* [2002] bilinear relation, Equation (2). Yellow line is *Wells and Coppersmith* [1994] scaling relation, Equation (4). Blue line is *Shaw* [2009] scaling relation, Equation (3). The S09′ relation is illustrated using default W values; solid blue line is $W = 15km$, dashed blue line is $W = 11km$.

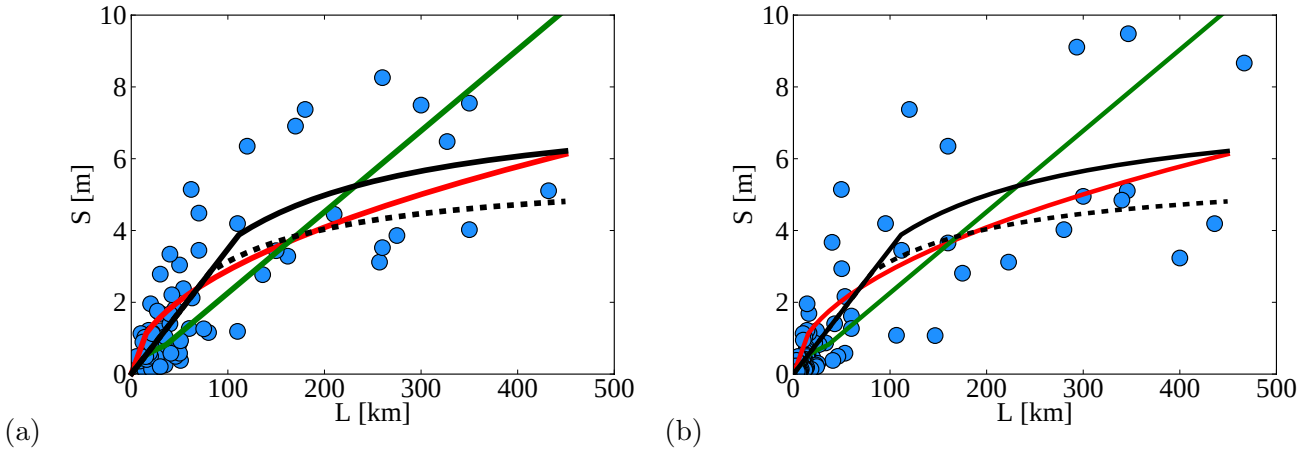

Figure 2: Fits of implied slip-length scaling by magnitude-area scalings. Magnitude is converted to moment, then divided by area and modulus to get slip. When length is available in database it is used. Otherwise area is converted to length by dividing area by width assuming seismogenic depth H=15 km. Data shown with light blue circles. Different color lines represent different magnitude-area scaling laws rescaled the same way the data has been. Parameters used directly from magnitude-area scaling laws, Table 2a. The curves are the implied slip-length for: Ellsworth-B [*WGCEP*, 2003] (red), Hanks-Bakun [*Hanks and Bakun*, 2008] (green), *Shaw* [2009] (black). The S09′ relation is illustrated using default W values; solid black line is $W = 15km$, dashed black line is $W = 11km$. (a) Data derived from WGCEP03 database. Event specific W's used. (b) Data derived from Hanks-Bakun database. Default $W = 15km$ used.

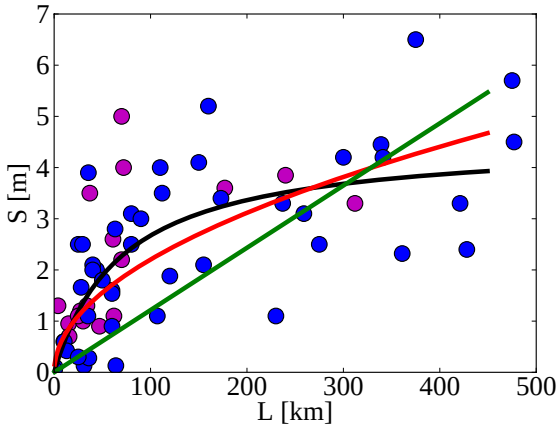

Figure 3: Fits of surface slip-length scaling laws to surface slip observations of average slip versus length using new *Biasi et al.* [2012] database. Color indicates focal mechanism: strike-slip (blue), dip-slip (magenta). Curves only fit to strike-slip data. In order of best fit to least good fit: black line shows Equation (13) constant stress drop scaling; red line shows Equation (10) $L^{1/2}$ scaling; green line shows Equation (11) L scaling. Note change in vertical axis scale in Figure 2 versus this Figure, reflecting overall systematic difference, and fundamental epistemic uncertainty, in average slip estimates from magnitude-area versus surface slip observations. Some of this difference reflects different events in the two different databases, but some of it, a difference of around 30%, remains when we restrict to looking at the same events. But also note overall qualitative consistency in trends of the two types of data in both figures.

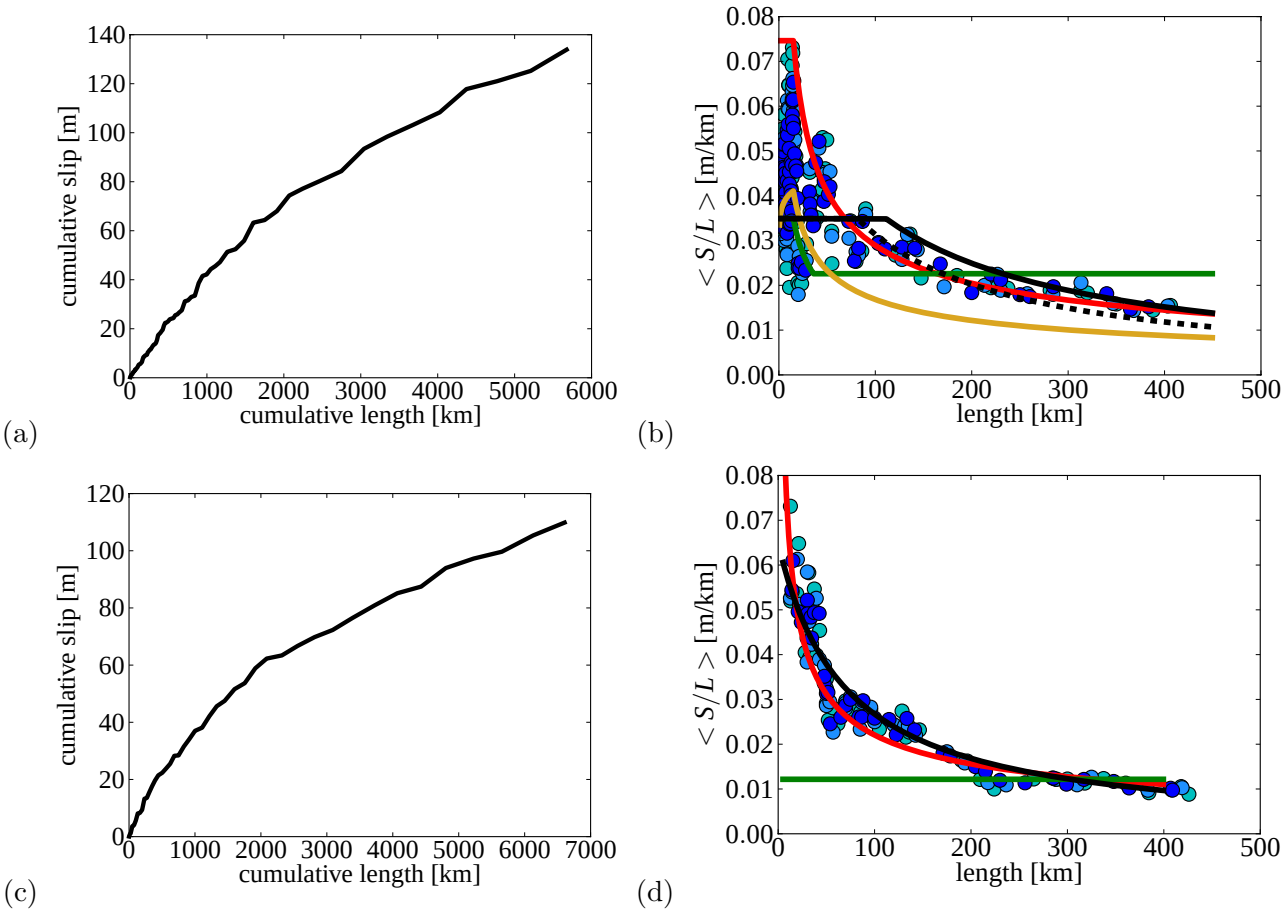

Figure 4: Sublinear scaling of slip with length. Top plots use implied slip-length from magnitude-area data. Bottom plots use surface slip-length data. (a) Cumulative slip versus cumulative length, showing the sub-linear scaling inherent in the data. Linear scaling would imply a straight line on the cumulative curve; downward curvature is sublinear scaling, increasing slower than linear, while upward curvature is supralinear scaling. increasing faster than linear. (b) Average slope given by local average slip over average length, plotted as a function of length. The local slope is fit by an average over n points in the neighborhood; here $n = 3, 4, 5$ in the different colors. The data are implied slip-length from the magnitude-are data of *Hanks and Bakun* [2008]. The different color curves show the different scaling laws fits. The curves are the implied slip-length derived from the magnitude area scaling relations: EB Equation (1) [red], WC Equation (4) [yellow], HB Equation (2) [green]. S09 Equation (3) [black]. The S09′ relation is shown with two default W values: $15km$ [solid black line], and $11km$ [dahed black line]. (c) Same as (a) but instead using surface slip data. (d) Same as (b) but instead using surface slip data. The different color curves show the different scaling laws fits, now for the surface slip relations. The data are surface slip-length *Biasi et al.* [2012]. The curves are $L^{1/2}$ Equation (10) [red], L Equation (11) [green], and constant stress drop Equation (13) [black].

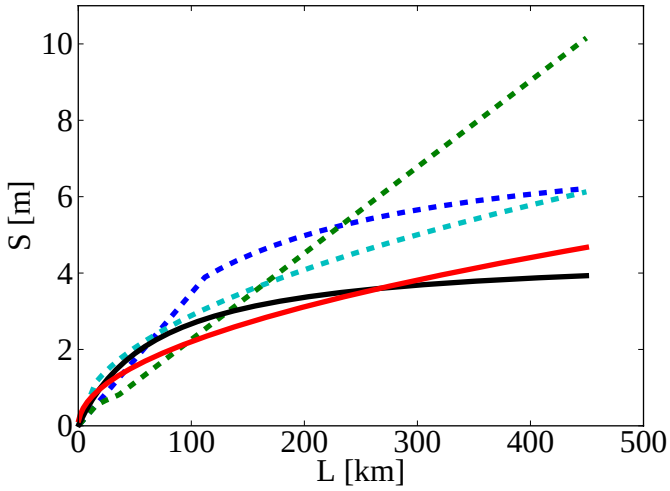

Figure 5: Slip length scaling relations for large strike-slip events. Dashed lines are implied slip-length scaling relations derived from Magnitude-Area scaling relations. Solid lines are slip-length scaling relations derived from surface slip observations. Note that the dashed lines are systematically above the solid lines at large lengths. Dashed lines from implied slip-length scaling parameters based on magnitude-area fits, Table 2a. Dashed cyan line is implied slip-length from Ellsworth-B [*WGCEP*, 2003] magnitude-area relation, Equation (1). Dashed blue line is implied slip-length from S09 Equation (3), illustrated using default $W = 15km$ value. Dashed green line is implied slip-length from *Hanks and Bakun* [2002] bilinear relation, Equation (2). Solid curves are fits to surface slip-length data. Solid red line is $L^{1/2}$ scaling, Equation (10). Solid black line is constant stress drop scaling [*Shaw*, 2013], Equation (13). The dashed blue line best fits the slip-length data derived from the magnitude-area data. The solid black line best fits the surface slip-length data.

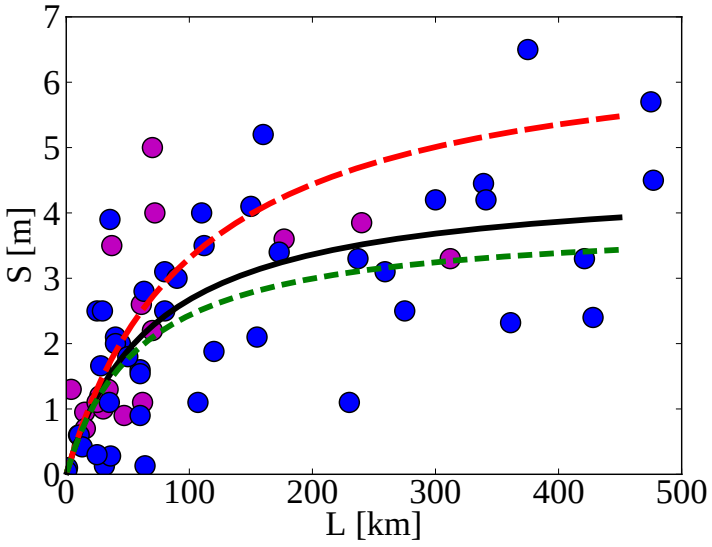

Figure 6: Dip effects on expected scaling. Data points are geological surface slip observations of average slip versus length from the new *Biasi et al.* [2012] database. Color indicates focal mechanism: strike-slip (blue), dip-slip (magenta). Solid lines show scaling expected for fixed seismogenic depth, but changing dip, and thus downdip width and changing modulus effects. All curves have the same stress drop, a value for best fit stress drop to strike-slip data of 4.54 MPa . Different curves use same seismogenic depth of $15km$ and different dips 90° (black) strike-slip Equation (13), and 60° (green) and 30° (red) dip-slip Equation (17). Note only relatively small differences expected in scaling of events with different focal mechanisms, which appears consistent with data.